

The Origin of Antibunching in Resonance Fluorescence

Lukas Hanschke,^{1,2,*} Lucas Schweickert,^{3,*} Juan Camilo López Carreño,^{4,*} Eva Schöll,³
Katharina D. Zeuner,³ Thomas Lettner,³ Eduardo Zubizarreta Casalengua,⁴ Marcus Reindl,⁵
Saimon Filipe Covre da Silva,⁵ Rinaldo Trotta,⁶ Jonathan J. Finley,^{2,7} Armando Rastelli,⁵
Elena del Valle,^{4,8} Fabrice P. Laussy,^{4,9} Val Zwiller,³ Kai Müller,^{1,2} and Klaus D. Jöns^{3,†}

¹*Walter Schottky Institut and Department of Electrical and Computer Engineering,
Technische Universität München, 85748, Garching, Germany*

²*Munich Center of Quantum Science and Technology (MCQST), 80799 Munich, Germany*

³*Department of Applied Physics, Royal Institute of Technology,
Albanova University Centre, Roslagstullsbacken 21, 106 91 Stockholm, Sweden*

⁴*Faculty of Science and Engineering, University of Wolverhampton,
Wulfruna St, Wolverhampton WV1 1LY, United Kingdom*

⁵*Institute of Semiconductor and Solid State Physics, Johannes Kepler University Linz, 4040, Austria*

⁶*Dipartimento di Fisica, Sapienza Università di Roma, Piazzale A. Moro 1, I-00185 Roma, Italy*

⁷*Walter Schottky Institut and Physik Department, Technische Universität München, 85748, Garching, Germany*

⁸*Departamento de Física Teórica de la Materia Condensada,
Universidad Autónoma de Madrid, 28049 Madrid, Spain*

⁹*Russian Quantum Center, Novaya 100, 143025 Skolkovo, Moscow Region, Russia*

(Dated: May 26, 2020)

Epitaxial quantum dots have emerged as one of the best single-photon sources, not only for applications in photonic quantum technologies but also for testing fundamental properties of quantum optics. One intriguing observation in this area is the scattering of photons with subnatural linewidth from a two-level system under resonant continuous wave excitation. In particular, an open question is whether these subnatural linewidth photons exhibit simultaneously antibunching as an evidence of single-photon emission. Here, we demonstrate that this simultaneous observation of subnatural linewidth and antibunching is not possible with simple resonant excitation. First, we independently confirm single-photon character and subnatural linewidth by demonstrating antibunching in a Hanbury Brown and Twiss type setup and using high-resolution spectroscopy, respectively. However, when filtering the coherently scattered photons with filter bandwidths on the order of the homogeneous linewidth of the excited state of the two-level system, the antibunching dip vanishes in the correlation measurement. Our experimental work is consistent with recent theoretical findings, that explain antibunching from photon-interferences between the coherent scattering and a weak incoherent signal in a skewed squeezed state.

Quantum dots are ideally suited as prototypical two-level quantum systems in the solid state. This is a result of their strong optical interband transitions, almost exclusive emission into the zero-phonon line and ease of integration into optoelectronic devices [1–4]. Moreover, the development of resonant excitation techniques [5], such as cross-polarized resonance fluorescence [6] has enabled nearly transform-limited linewidths [7], as the resonant excitation avoids the generation of free charge carriers which can lead to a fluctuating electronic environment resulting in spectral diffusion [8]. This technique has enabled multiple exciting tests of quantum optics as well as the use of quantum dots as sources of non-classical light for photonic quantum technologies [4]. For example, using pulsed excitation, Rabi oscillations have been demonstrated and enabled the on-demand generation of single photons [9], entangled photon pairs [10], two-photon pulses [11], and photon number superposition states [12]. Furthermore, continuous wave excitation has led to the observation of Mollow triplets for strong driving [13] as well as coherent Rayleigh scattering in the regime of weak driving [14–16]. In the latter case, light is coherently scattered by the two-level system leading to a subnatural linewidth of the photons which inherit the coherence of the laser [17]. While previous experimental works have indicated that the coherently scattered light

exhibits antibunching [14, 15], recent theoretical studies have predicted that the antibunching is only enabled by the presence of weak incoherent emission interfering with the coherently scattered light [18]. Therefore, it was predicted that selectively transmitting the narrow coherent scattering by frequency filtering, i.e., suppressing the incoherently scattered component, would inhibit the observation of antibunching. In this letter, we experimentally test this prediction and observe that, indeed, it is only possible to observe either subnatural linewidth or antibunching under simple resonant excitation. We provide a fundamental theoretical model giving insight to the underlying mechanism which agrees very well with our experimental results without data processing. The excellent accord between experiment and theory indicates that targeted experiments to control the balance of coherent and incoherent fractions and simultaneously achieve antibunching and subnatural linewidth, are within sight.

The quantum dots used in this study were grown by droplet etch epitaxy [19, 20]. An aluminum droplet is used to dissolve an AlGaAs substrate at distinct positions to form near perfectly round holes with a diameter of ~ 100 nm and ~ 5 nm depth. These holes are filled with GaAs in a second step and capped again by AlGaAs to form single quantum dots. A frequency tunable diode laser with a narrow linewidth of 50 kHz

is used to resonantly excite a single quantum dot. To suppress the leakage of laser light into the detection path of the setup we use a pair of perpendicular thin film polarizers in the excitation and detection paths. The emitted photons are further filtered with a self-build transmission spectrometer with a FWHM of 19 GHz to suppress any residual emission of other transitions. Figure 1 a) depicts the setup used for this experiment which can be used either to introduce a Hanbury Brown and Twiss setup to investigate the photon statistics or a scanning Fabry-Pérot cavity to obtain high resolution spectra. By populating higher excited states of the quantum dot with a laser that is at the same time mixed with low intensity white light to stabilize the electrical environment [21] we obtain the spectrum shown in Fig. 1 b). Several emission lines appear, among which we can identify the neutral exciton transition. Switching to resonant excitation leads to a clean spectrum with only a single peak from the excited transition, shown in Fig. 1 c).

We now focus on studying the emission under resonant excitation using a scanning Fabry-Pérot interferometer with a spectral resolution of 28 MHz. While in a linear scale (Fig. 2 a)) the spectrum seems to consist of only one sharp peak, a plot in logarithmic scale (Fig. 2 b)) reveals the presence of two superimposed peaks: A sharp peak with a linewidth of 28 MHz and a broader peak with a linewidth of (890 ± 60) MHz. While the sharp peak stems from the coherent scattering and is only limited by the resolution of the scanning Fabry-Pérot interferometer, the broader peak stems from incoherent emission. Here, the observed linewidth results from emission mainly given by the Fourier-limit. The ratio of the integrated peak areas is 1:2.65 and consistent with the numerical simulation of a resonantly driven two-level system (Fig. 2 c)) where for weak driving the coherent scattering dominates while for strong driving the situation is reversed.

To verify the single-photon character of the quantum dot emission, we perform second order intensity autocorrelation measurements using a Hanbury Brown and Twiss setup connected to two superconducting nanowire single-photon detectors, with low dark count rates [22]. Our Hanbury Brown and Twiss setup has a time resolution of 70 ps given by the internal response function. The unfiltered emission in the Rayleigh regime shows near perfect antibunching Fig. 3 (red), confirming the single-photon character, with a measured degree of second-order coherence of $g^{(2)}(0) = 0.022 \pm 0.011$. For this measurement we used a broad frequency filter of FWHM = 19 GHz, more than 20 times broader than the linewidth of the incoherent emission.

The light emitted by an ideal two-level system under perfect detection conditions is always antibunched, but the physical mechanism for this depends on the regime in which it is being excited. In the case of coherent driving by a laser, one can distinguish between the weak-driving Rayleigh regime where antibunching is due to a coherent process of absorption and re-emission of the incident coherent radiation by the two-level system [23], and the strong-driving limit, where the two-level system blocks the excitation, gets saturated and emits antibunched light in the fashion of the spontaneous emission of

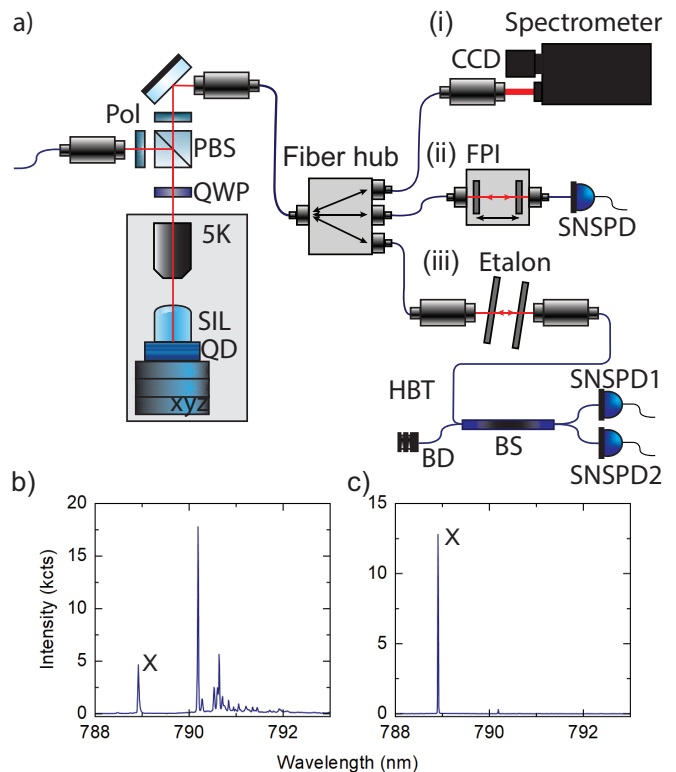


FIG. 1. a) Experimental setup to generate coherently scattered photons from our GaAs quantum dot. Cross polarization using a polarizing beam splitter (PBS), nano particle polarizers (Pol) and a quarter waveplate (QWP). The photons scattered from the quantum dot are additionally spatially filtered from the excitation laser using a single-mode fiber. The quantum dot is located in a closed-cycle cryostat at 5 K temperature. A solid immersion lens (SIL) increases the collection efficiency of the emitted quantum light. The collected signal can be analyzed (i) in a spectrometer equipped with a silicon CCD, (ii) using a tunable Fabry-Pérot interferometer (FPI) equipped with a superconducting nanowire single-photon detector (SNSPD), or (iii) by sending it through different types of frequency filters (Etalon) and then into a Hanbury Brown and Twiss (HBT) setup to measure the second-order intensity autocorrelation of the signal (BD = beam dump, BS = 50/50 beam splitter). b) Quasi-resonant excitation spectrum of the investigated quantum dot, using 781 nm wavelength pulsed excitation. c) Resonance fluorescence spectrum of the same quantum dot as graph b). The exciton (X) is excited resonantly with a narrow-band continuous wave diode laser.

a two-level system. While one has in mind the second mechanism when thinking of antibunching from a two-level system, the first mechanism is completely unrelated and must be understood instead as an interference effect [24]. The two-level system annihilation operator σ can be decomposed into a sum of a coherent term $\langle \sigma \rangle$ and a quantum, or incoherent, term $\zeta \equiv \sigma - \langle \sigma \rangle$ as:

$$\sigma = \langle \sigma \rangle + \zeta. \quad (1)$$

Note that ζ is an operator, like σ , in fact it is simply σ minus its coherent part $\langle \sigma \rangle$. Their respective intensities as a function

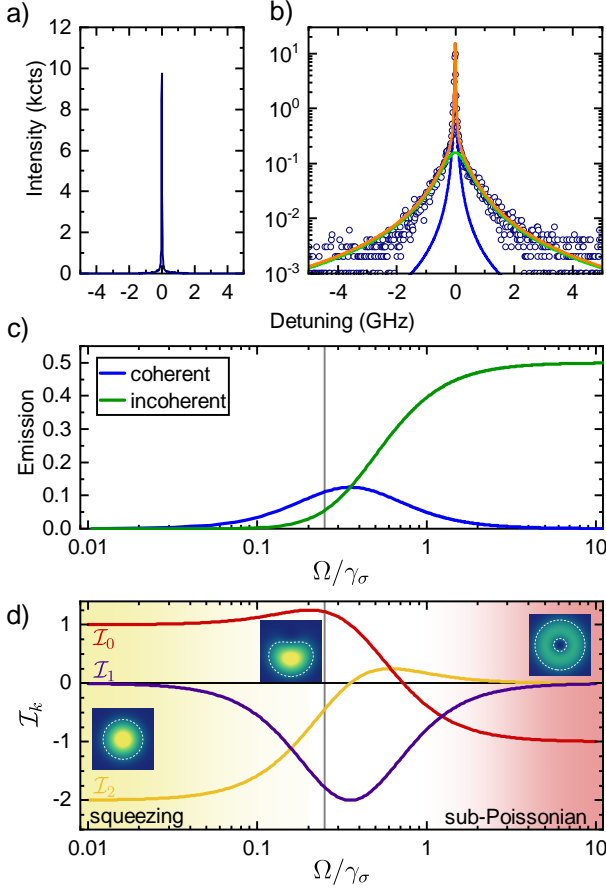


FIG. 2. a) High resolution spectrum of the exciton transition under resonant excitation in the weak pumping regime. b) The spectrum plotted in semi-logarithmic scale reveals a second broader peak. Blue line: coherently scattered laser, green line: incoherent resonance fluorescence; orange line: cumulative peak. c) Theoretical curve of the intensity of the coherent and incoherent component as a function of the driving power. d) Two-photon interference terms I_k , Eqs. (4), with $k = 0, 2$ playing a role at weak and strong drivings and showing how antibunching $g^{(2)}(0) = 0$ arises from squeezing (with $I_2 = -2$ on the left) or sub-Poissonian statistics of the emitter (with $I_0 = -1$, on the right). The transition between the two regimes occurs through a skewing of the squeezed state whereby I_2 gets replaced by I_1 . Insets: the Wigner representation $W_\sigma(X, Y)$ of the quantum state at weak, intermediate and strong driving, for $-1.5 \leq X, Y, \leq 1.5$ with white dashed isolines at 0 and 0.1. Note that at strong driving, W_σ becomes negative (non-Gaussian). The vertical line indicates the driving of our experiment.

of the driving Ω and emission rate γ_σ are given by [25]:

$$|\langle \sigma \rangle|^2 = \frac{4\gamma_\sigma^2 \Omega^2}{(\gamma_\sigma^2 + 8\Omega^2)^2} \quad \text{and} \quad \langle \zeta^\dagger \zeta \rangle = \frac{32\Omega^4}{(\gamma_\sigma^2 + 8\Omega^2)^2} \quad (2)$$

and are shown in Fig. 2(c). While the total intensity $n_\sigma \equiv \langle \sigma^\dagger \sigma \rangle$ for the sum of these two fields would typically involve an interference term $n_\sigma = |\langle \sigma \rangle|^2 + \langle \zeta^\dagger \zeta \rangle + 2\text{Re}(\langle \sigma \rangle^* \langle \zeta \rangle)$, in this case there is no interference since $\langle \zeta \rangle = 0$ by construction (ζ has no mean field). Higher-order photon correlations,

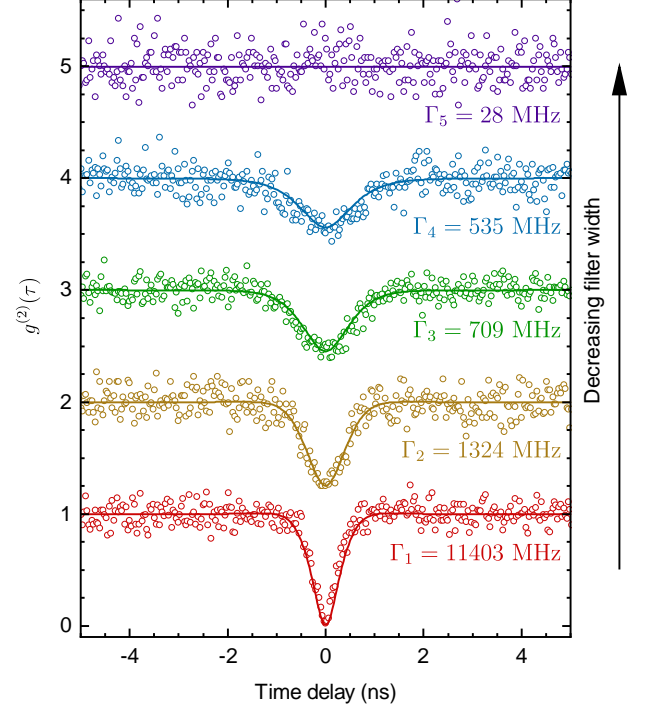


FIG. 3. Second-order intensity correlation function $g^{(2)}(\tau)$ of the quantum dot emission in the Rayleigh regime for different spectral filter widths Γ_x . With decreasing filter width, a larger portion of the incoherent component is suppressed, unbalancing the two-photon interference which produces antibunching in this regime. The experimental data is shown with empty circles, while the solid lines are obtained with the theory of frequency-resolved correlations using the parameters given in Table I.

however, do exhibit such interferences between the coherent component $\langle \sigma \rangle$, which inherits the statistics of the laser, and ζ , which follows the statistics of the two-level system's quantum fluctuations. Such interferences, at the two-photon level, are quantified by coefficients I_k which add up to the zero-delay two-photon coherence function $g^{(2)}(0)$ as follows [26–28]:

$$g^{(2)}(0) = 1 + I_0 + I_1 + I_2, \quad (3)$$

where:

$$I_0 = \frac{\langle \zeta^{\dagger 2} \zeta^2 \rangle - \langle \zeta^\dagger \zeta \rangle^2}{\langle \sigma^\dagger \sigma \rangle^2}, \quad (4a)$$

$$I_1 = 4 \frac{\Re[\langle \sigma \rangle^* \langle \zeta^\dagger \zeta^2 \rangle]}{\langle \sigma^\dagger \sigma \rangle^2}, \quad (4b)$$

$$I_2 = \frac{\langle X_{\zeta, \phi}^2 \rangle - \langle X_{\zeta, \phi} \rangle^2}{\langle \sigma^\dagger \sigma \rangle^2}, \quad (4c)$$

and $X_{\zeta, \phi} = (e^{i\phi} \zeta^\dagger + e^{-i\phi} \zeta)/2$ is the ζ -field quadrature. I_0 describes the sub-Poissonian (when negative) or super-Poissonian (when positive) character of the quantum fluctuations, I_1 its so-called anomalous moments [26, 28] and I_2 its

squeezing [29] (when negative). These quantities are shown in Fig. 2 d), where one can see the transition from $\mathcal{I}_0 = 1$ to -1 when going from weak to strong driving, which is compensated by the transition from $\mathcal{I}_2 = -2$ to 0 to keep the total (3) zero. To keep this identically zero also in the transition between these two regimes, the system develops a skewness in its squeezing through the anomalous correlation term \mathcal{I}_1 that overtakes \mathcal{I}_2 , with $\langle \zeta^\dagger \zeta^2 \rangle$ becoming non-zero (it cannot be factored into $\langle \zeta^\dagger \zeta \rangle \langle \zeta \rangle$ anymore), in such a way as to satisfy $\mathcal{I}_1 = -(1 + \mathcal{I}_0 + \mathcal{I}_2)$ [24]. The numerator $\Re[\langle \sigma \rangle^* \langle \zeta^\dagger \zeta^2 \rangle]$ can be written as $|\langle \sigma \rangle| (\langle : X_{\zeta, \phi}^3 : \rangle + \langle : X_{\zeta, \phi} Y_{\zeta, \phi}^2 : \rangle)$ with $Y_{\zeta, \phi} \equiv \frac{i}{2} (e^{i\phi} \zeta^\dagger - e^{-i\phi} \zeta)$ the other ζ -quadrature and $::$ denoting normal-ordering of the enclosed quantity. This shows that, at weak driving, \mathcal{I}_1 becomes nonzero when the quantum state departs from a Gaussian description (squeezed thermal state) in the transition to the strong driving regime where it acquires the full non-Gaussian character of a single-photon source that is produced by a Fock state. Indeed, the full emission at strong driving comes exclusively from the quantum part $\sigma \approx \zeta$, with the system getting into the statistical mixture $\rho = \frac{1}{2}(|0\rangle\langle 0| + |1\rangle\langle 1|)$, with no coherence involved, $\langle \sigma \rangle = 0$. Accordingly, the sub-Poissonian statistics reaches its minimum $\mathcal{I}_0 = -1$. In the weak driving regime, antibunching is, on the opposite, due to squeezing of the quantum fluctuations ζ , with the system being in a pure or skewed squeezed thermal state, with either \mathcal{I}_2 or \mathcal{I}_1 being -2 , interfering with the coherent component $\langle \sigma \rangle$ to produce $g^{(2)}(0) = 0$. This is even more clearly illustrated by considering the Wigner representation of the quantum state, as shown by the insets in Fig. 2 d) in the three regimes of interest, where one can see how the system evolves from a Gaussian state (a displaced squeezed thermal state) to a Fock state (a ring with a distribution that admits negative values) passing by a skewed (bean-shaped) Wigner distribution at the point of our experiment. Note that in the weak-driving regime, both the displacement and the ellipticity of the displaced squeezed thermal state are too small to be seen compared to the dominant thermal distribution, but both are necessary to produce antibunching. Counter-intuitively, at weak and intermediate driving, in direct opposition to the strong-driving case, quantum fluctuations are in fact super-Poissonian, with $\mathcal{I}_0 \geq 1$. It is the interference between such superbunched quantum fluctuations with the coherence of the mean-field that result in an overall antibunching, this being the two-photon counterpart of the apparent paradox of two waves adding to produce no signal (destructive interferences). This understanding of the nature of antibunching in the Rayleigh regime is important because attributing the non-Gaussian antibunching to the scattered light makes it tempting to regard the scattered light as having both the spectral feature of the laser, with a narrow linewidth, and the statistical property of a two-level system, antibunched. It has, indeed, been hailed as such in the literature [14, 15]. As we have shown, however, the Rayleigh antibunching does not come from the two-level character of the emitter, which is not involved at such weak drivings, but from the interference between the mean-field $\langle \sigma \rangle$ as driven by the laser (coherent ab-

sorption) and the quantum fluctuations $\sigma - \langle \sigma \rangle$ (incoherent re-emission). Because it is due to some interference, any tampering with the balance $\mathcal{I}_0 + \mathcal{I}_1 + \mathcal{I}_2 = -1$, for instance by frequency filtering, will result in spoiling the antibunching $g^{(2)}(0) = 0$. Filtering is a fundamental process in any quantum-optical measurement, since beyond the finite bandwidth of any physical detector, a measurement that is accurate in time requires detections at all frequencies and, vice-versa, spectrally resolving emission requires integration over time. To challenge the naive picture that light coherently-scattered from a two-level system is antibunched, we measure $g^{(2)}(\tau)$ for decreasing filter widths that increasingly isolate the coherent component. According to this naive picture, this should not affect the property of light since the ‘‘single photons’’ are spectrally sharp and will pass through the filter which does not block at their frequency. According to the Rayleigh picture of interferences, however, this will disrupt the balance of the \mathcal{I}_k coefficients in their two-photon interference to produce antibunching. The theory shows that, for zero-delay coincidences in the weak-driving regime, the coefficients vary as a function of filtering Γ as [30]:

$$\mathcal{I}_0 = \frac{\Gamma^2}{(\Gamma + \gamma_\sigma)^2}, \quad \mathcal{I}_1 = 0, \quad \mathcal{I}_2 = -\frac{2\Gamma}{\Gamma + \gamma_\sigma}, \quad (5)$$

with, therefore (cf. Eq. (3))

$$g^{(2)}(0) = \left(\frac{\gamma_\sigma}{\Gamma + \gamma_\sigma} \right)^2. \quad (6)$$

As these expressions show, filtering affects more the ζ statistics than it does affect the squeezing of its quadratures. This behaviour can be reproduced in the experiment by inserting a narrow spectral filter in the detection path. Measurements of $g^{(2)}(\tau)$ for different filter widths of (1550 ± 320) MHz, (780 ± 160) MHz, (390 ± 80) MHz and 28 MHz are presented as yellow, green, blue and purple data points in Fig. 3, respectively. The data are offset in vertical direction for clarity. Clearly, with decreasing filter width, the depth of the antibunching dip decreases until it completely vanishes.

This is in excellent agreement with our theoretical model, that describes finite τ -delay coincidences of the filtered light with an exact theory of time- and frequency-resolved photon correlations [31]. This provides an essentially perfect quantitative agreement with the data without any processing such as deconvolution, provided, however, that one also includes the effect of the anomalous moment term \mathcal{I}_1 which bridges between the weak and strong driving regimes. Indeed, Ω was not so low in the experiment—in the interest of collecting enough signal in presence of filtering—as to realize an ideal squeezed state to interfere with the coherent fraction to produce the antibunching, but relied on a distorted, skewed version of the squeezed state in its transition towards the non-Gaussian, strong-driving regime where squeezing has disappeared altogether. This term brings quantitative deviations which are necessary to take into account to provide an exact match with the

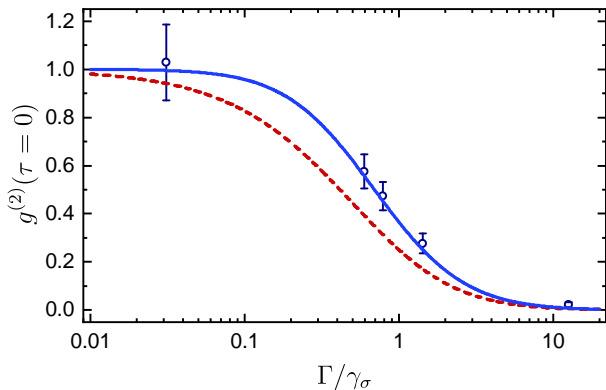


FIG. 4. Loss of antibunching in the Rayleigh regime due to filtering Γ . Dashed-red line, the limit of vanishing driving, Eq. (6), and solid-blue line, the case of small but finite driving Ω , Eq. (20). Our experimental data fits perfectly with the theoretical prediction.

Parameter	γ_σ	Ω	Γ_1	Γ_2	Γ_3	Γ_4	Γ_5
Fitting (MHz)	900	225	11403	1324	709	535	28
Data (MHz)	890	198	19000	1550	780	390	28
(Error)	(60)	(7)	(500)	(320)	(160)	(80)	(6)

TABLE I. Summary of the parameters used to fit the experimental data. The filters data are taken from the fabricant's data sheet, but are known to be typically measured in excess of their specified value.

data. The unfiltered case, for instance, sees the vanishing-driving two-photon statistics $g^{(2)}(\tau) = [1 - \exp(-\gamma_\sigma \tau/2)]^2$ turn into

$$g^{(2)}(\tau) = 1 - e^{-3\gamma_\sigma \tau/4} \left[\cosh\left(\frac{R\tau}{4}\right) + \frac{3\gamma_\sigma}{R} \sinh\left(\frac{R\tau}{4}\right) \right], \quad (7)$$

at non-negligible driving, with $R = \sqrt{\gamma_\sigma^2 - 64\Omega^2}$. Using this and numerically-exact filtered counterparts, with a global fitting that only varies the filters widths and globally optimises the driving strength Ω and the two-level's decay rate $\gamma_\sigma = 900$ MHz (cf. Table I), we obtain the solid lines shown in Fig. 3, providing an excellent quantitative agreement with highly constrained fitting parameters. From this data, one can extract the zero-delay coincidence and compare it to the theory, i.e., both Eq. (6), shown in dashed Red in Fig. 4, or to the finite Ω counterpart that skews the squeezing, and whose expression is too bulky to be written here [32], but is given in the Supplementary Material, Eq. (20). This also yields an excellent agreement with the experimental data, which confirms that filtering spoils antibunching according to the scenario we have explained of perturbing the interference of the squeezed fluctuations with the coherent signal, and that the experiment is clean and fundamental enough to be reproduced exactly by including non-vanishing driving features, without any further signal analysis or data processing.

In summary, we have shown that the emission from a two-level quantum system driven in the Rayleigh regime does not

simultaneously yield subnatural linewidth and single-photon characteristics. When keeping only the subnatural linewidth part of the spectrum by frequency filtering, we do not observe antibunching in our second-order intensity correlation measurement. The narrower the spectral filtering, i.e., the fewer incoherently scattered photons we detect, the weaker the antibunching dip, which ultimately results in Poissonian photon statistics. These results that disclose a perfect agreement with a fundamental theory of time and frequency resolved photon correlations, with no post-processing of the raw experimental data, are only the first step towards a full exploitation of its consequences. In particular, since the interference involves a coherent field, it is technically possible to restore it fully in presence of filtering or, which is equivalent, detection, simply by introducing externally the coherent fraction that is missing or, in this case, in excess. This is done by destructive interferences of the coherent signal, without perturbing the quantum fluctuations. As a result, one should indeed obtain a subnatural, laser-sharp, photon emission that is also perfectly antibunched [18]. There are still other interesting features in this regime, such as a plateau in the time-resolved photon correlations. Such considerable improvements are in the wake of our present findings.

Note added after proof: During the submission/preparation of the manuscript we became aware of a similar work [33].

This project has received funding from the European Union's Horizon 2020 research and innovation program under grant agreement No. 820423 (S2QUIP), the European Research Council (ERC) under the European Union's Horizon 2020 Research and Innovation Programme (SPQReI, grant agreement no. 679183), Austrian Science Fund (FWF): P 29603, P 30459, the Linz Institute of Technology (LIT) and the LIT Lab for secure and correct systems, supported by the State of Upper Austria, the German Federal Ministry of Education and Research via the funding program Photonics Research Germany (contract number 13N14846), Q.Com (Project No. 16KIS0110) and Q.Link.X (16KIS 0874), the DFG via Project (SQAM) F1947/4-1, the Nanosystem Initiative Munich, the MCQST, the Knut and Alice Wallenberg Foundation grant "Quantum Sensors", the Swedish Research Council (VR) through the VR grant for international recruitment of leading researchers (Ref: 2013-7152), and Linnæus Excellence Center ADOPT. K.M. acknowledges support from the Bavarian Academy of Sciences and Humanities. K.D.J. acknowledges funding from the Swedish Research Council (VR) via the starting Grant HyQRep (Ref 2018-04812) and The Göran Gustafsson Foundation (SweTeQ). A.R. acknowledges fruitful discussions with Y. Huo, G. Weihs, R. Keil and S. Portalupi.

* L. H., L. S. and J. C. L. C. contributed equally to this work

† corresponding author: klausj@kth.se

[1] R. Trivedi, K. A. Fischer, J. Vučković, and K. Müller, *Advanced*

- Quantum Technologies **3**, 1900007 (2020).
- [2] P. Borri, W. Langbein, S. Schneider, U. Woggon, R. L. Sellin, D. Ouyang, and D. Bimberg, *Physical Review Letters* **87**, 157401 (2001).
- [3] A. J. Brash, J. Iles-Smith, C. L. Phillips, D. P. McCutcheon, J. O'Hara, E. Clarke, B. Royall, L. R. Wilson, J. Mørk, M. S. Skolnick, A. M. Fox, and A. Nazir, *Physical Review Letters* **123**, 167403 (2019).
- [4] P. Senellart, G. Solomon, and A. White, *Nature Nanotechnology* **12**, 1026 (2017).
- [5] A. Muller, E. B. Flagg, P. Bianucci, X. Y. Wang, D. G. Deppe, W. Ma, J. Zhang, G. J. Salamo, M. Xiao, and C. K. Shih, *Physical Review Letters* **99**, 187402 (2007).
- [6] A. V. Kuhlmann, J. Houel, D. Brunner, A. Ludwig, D. Reuter, A. D. Wieck, and R. J. Warburton, *Review of Scientific Instruments* **84**, 073905 (2013).
- [7] A. V. Kuhlmann, J. H. Prechtel, J. Houel, A. Ludwig, D. Reuter, A. D. Wieck, and R. J. Warburton, *Nature Communications* **6**, 8204 (2015).
- [8] D. Chen, G. R. Lander, K. S. Krowpman, G. S. Solomon, and E. B. Flagg, *Physical Review B* **93**, 115307 (2016).
- [9] Y. M. He, Y. He, Y. J. Wei, D. Wu, M. Atatüre, C. Schneider, S. Höfling, M. Kamp, C. Y. Lu, and J. W. Pan, *Nature Nanotechnology* **8**, 213 (2013).
- [10] M. Müller, S. Bounouar, K. D. Jöns, M. Glässl, and P. Michler, *Nature Photonics* **8**, 224 (2014).
- [11] K. A. Fischer, L. Hanschke, J. Wierzbowski, T. Simmet, C. Dory, J. J. Finley, J. Vučković, and K. Müller, *Nature Physics* **13**, 649 (2017).
- [12] J. C. Loredó, C. Antón, B. Reznichenko, P. Hilaire, A. Harouri, C. Millet, H. Ollivier, N. Somaschi, L. De Santis, A. Lemaitre, I. Sagnes, L. Lanco, A. Auffèves, O. Krebs, and P. Senellart, *Nature Photonics* **13**, 803 (2019).
- [13] E. B. Flagg, A. Muller, J. W. Robertson, S. Founta, D. G. Deppe, M. Xiao, W. Ma, G. J. Salamo, and C. K. Shih, *Nature Physics* **5**, 203 (2009).
- [14] H. S. Nguyen, G. Sallen, C. Voisin, P. Roussignol, C. Diederichs, and G. Cassabois, *Applied Physics Letters* **99**, 261904 (2011).
- [15] C. Matthiesen, A. N. Vamivakas, and M. Atatüre, *Physical Review Letters* **108**, 093602 (2012).
- [16] K. Konthasinghe, J. Walker, M. Peiris, C. K. Shih, Y. Yu, M. F. Li, J. F. He, L. J. Wang, H. Q. Ni, Z. C. Niu, and A. Muller, *Physical Review B - Condensed Matter and Materials Physics* **85**, 235315 (2012).
- [17] C. Matthiesen, M. Geller, C. H. Schulte, C. Le Gall, J. Hansom, Z. Li, M. Hugues, E. Clarke, and M. Atatüre, *Nature Communications* **4**, 1600 (2013).
- [18] J. C. López Carreno, E. Zubizarreta Casalengua, F. P. Laussy, and E. Del Valle, *Quantum Science and Technology* **3**, 4 (2018).
- [19] C. Heyn, A. Stemmann, T. Köppen, C. Strelow, T. Kipp, M. Grave, S. Mendach, and W. Hansen, *Applied Physics Letters* **94**, 183113 (2009).
- [20] Y. H. Huo, A. Rastelli, and O. G. Schmidt, *Applied Physics Letters* **102**, 152105 (2013).
- [21] H. S. Nguyen, G. Sallen, C. Voisin, P. Roussignol, C. Diederichs, and G. Cassabois, *Physical Review Letters* **108**, 057401 (2012).
- [22] L. Schweickert, K. D. Jöns, K. D. Zeuner, S. F. Covre Da Silva, H. Huang, T. Lettner, M. Reindl, J. Zichi, R. Trotta, A. Rastelli, and V. Zwiller, *Applied Physics Letters* **112**, 093106 (2018).
- [23] W. Heitler, *The quantum theory of radiation* (Oxford University Press, London, 1954).
- [24] E. Zubizarreta Casalengua, J. C. López Carreño, F. P. Laussy, and E. del Valle, *Laser Photon. Rev.* **1900279** (2020), 10.1002/lpor.201900279.
- [25] P. Meystre and M. Sargent, *Elements of Quantum Optics* (Springer, 2007) pp. 1–507.
- [26] L. Mandel, *Physical Review Letters* **49**, 136 (1982).
- [27] H. J. Carmichael, *Physical Review Letters* **55**, 2790 (1985).
- [28] W. Vogel, *Physical Review Letters* **67**, 2450 (1991).
- [29] R. Loudon, *The quantum theory of light* (Oxford University Press, 2000).
- [30] E. Zubizarreta Casalengua, J. C. López Carreño, F. P. Laussy, and E. del Valle, *Phys. Rev. A*, in press (2020), arXiv:2004.11885.
- [31] E. Del Valle, A. Gonzalez-Tudela, F. P. Laussy, C. Tejedor, and M. J. Hartmann, *Physical Review Letters* **109**, 183601 (2012).
- [32] J. C. López Carreño and F. P. Laussy, *Physical Review A* **94**, 063825 (2016).
- [33] C. L. Phillips, A. J. Brash, D. P. S. McCutcheon, J. Iles-Smith, E. Clarke, B. Royall, M. S. Skolnick, A. M. Fox, and A. Nazir, (2020), arXiv:2002.08192.
- [34] R. J. Glauber, *Physical Review Letters* **10**, 84 (1963).

**THE ORIGIN OF ANTIBUNCHING IN RESONANCE FLUORESCENCE
SUPPLEMENTARY MATERIAL**

The theoretical description of a coherently driven quantum dot modelled as a two-level system is straightforward with the formalism of open quantum systems, e.g., writing the master equation (we take $\hbar = 1$)

$$\partial_t \rho = i[\rho, H_\sigma] + (\gamma_\sigma/2)\mathcal{L}_\sigma \rho, \quad (8)$$

where $H_\sigma = \Delta_\sigma \sigma^\dagger \sigma + \Omega(\sigma^\dagger + \sigma)$ is the Hamiltonian of the quantum dot, with the two-level system annihilation operator σ driven by a laser with (c -number) intensity Ω with a detuning Δ_σ , which is zero in the conditions of our experiment (resonance). The spontaneous decay of the quantum dot is modeled by the rightmost term in Eq. (8), where γ_σ is the decay rate and $\mathcal{L}_c = (2c\rho c^\dagger - \rho c^\dagger c - c^\dagger c\rho)$. Standard techniques yield the steady-state of Eq. (8) which is

$$\rho = (1 - n_\sigma) |0\rangle\langle 0| + \langle\sigma\rangle |0\rangle\langle 1| + \langle\sigma\rangle^* |1\rangle\langle 0| + n_\sigma |1\rangle\langle 1|, \quad (9)$$

where the total population n_σ and mean field $\langle\sigma\rangle$ are

$$n_\sigma = \frac{4\Omega^2}{\gamma_\sigma^2 + 4\Delta_\sigma^2 + 8\Omega^2} \quad \text{and} \quad \langle\sigma\rangle = \frac{2i\Omega(\gamma_\sigma - 2i\Delta_\sigma)}{\gamma_\sigma^2 + 4\Delta_\sigma^2 + 8\Omega^2}. \quad (10)$$

Equations (9–10) convey well how n_σ relates to the incoherent relaxation in the sense of the two-level system being excited or spontaneously emitting (diagonal elements of the density matrix) and how $\langle\sigma\rangle$ relates to a coherent scattering connecting the ground and excited states (off-diagonal elements). The case $\Delta_\sigma = 0$ recovers Eqs. (2) of the text and their relative ratio as a function of pumping power Ω is shown in Fig. 2(c). A useful and standard representation of the density matrix ρ is the Wigner quasiprobability distribution

$$\tilde{W}(x, p) \equiv \frac{1}{\pi} \int_{-\infty}^{\infty} \langle x+y | \rho | x-y \rangle e^{-2ipy} dy, \quad (11)$$

where x and p represent two conjugate observables which, in our case, are proportional to the quantities of eventual interest, namely the orthogonal set of (averaged) field quadratures X and Y (that is, ‘position’ is $x = \sqrt{2}X$ while ‘momentum’ is $p = \sqrt{2}Y$). Consequently, $|x\rangle$ is the eigenstate that corresponds to the ‘position’ operator. By substituting Eq. (9) into (11), one gets

$$\tilde{W}_\sigma(x, p) = (1 - n_\sigma) \tilde{W}_{00} + \langle\sigma\rangle \tilde{W}_{01} + \langle\sigma\rangle^* \tilde{W}_{10} + n_\sigma \tilde{W}_{11}, \quad (12)$$

where \tilde{W}_{mn} are the Wigner representations of the Fock state matrix elements $|m\rangle\langle n|$:

$$\tilde{W}_{mn} = \frac{1}{\pi} \int_{-\infty}^{\infty} \psi_m^*(x+y) \psi_n(x-y) e^{-2ipy} dy. \quad (13)$$

Within the integrand, the ‘position’ representation of the number-states $|m\rangle$ is:

$$\psi_m(x) = \langle x | m \rangle = \sqrt{\frac{1}{2^m m! \sqrt{\pi}}} e^{-x^2/2} H_m(x), \quad (14)$$

where $H_m(x)$ are the Hermite polynomials. After integration, we obtain the next expressions:

$$\tilde{W}_{00} = \frac{1}{\pi} e^{-(x^2+p^2)}, \quad (15a)$$

$$\tilde{W}_{01} = \tilde{W}_{10}^* = \frac{\sqrt{2}}{\pi} (x+ip) e^{-(x^2+p^2)}, \quad (15b)$$

$$\tilde{W}_{11} = \frac{1}{\pi} (2x^2 + 2p^2 - 1) e^{-(x^2+p^2)}. \quad (15c)$$

We finally express the Wigner distribution in terms of the quadratures of interest by changing $x \rightarrow \sqrt{2}X$ and $p \rightarrow \sqrt{2}Y$ so the Wigner distribution reads:

$$W_\sigma(X, Y) = 2 \tilde{W}_\sigma(\sqrt{2}X, \sqrt{2}Y). \quad (16)$$

The factor 2 is to preserve the normalization condition for the Wigner distribution. The representation W_σ is for the full state σ . It is simply related to W_ζ the representation of the fluctuations by a mere translation in phase-space:

$$W_\zeta(X, Y) = W_\sigma(X - \Re\langle\sigma\rangle, Y - \Im\langle\sigma\rangle) \quad (17)$$

since σ and ζ are themselves related by the addition of a coherent state $\sigma = \zeta + \langle\sigma\rangle$. Therefore, the shape of the distribution is the same for both σ and ζ . Furthermore, in the Rayleigh regime of weak-driving, although $\langle\sigma\rangle$ dominates over n_σ according to Eq. (10), it is so small as to produce a negligible displacement of the Gaussian cloud, itself in a thermal squeezed state, which in appearance looks like a thermal state, since squeezing is too small compared to the thermal component to be seen with the naked eye. It is, however, essential to produce antibunching as a thermal and coherent admixture can only produce two-photon statistics between 1 and 2. In the Fock regime of strong-driving, $\langle\sigma\rangle = 0$ and $W_\sigma = W_\zeta$ exactly. In the intermediate case, the bean-shaped skewed Wigner distribution is translated downward as the result of sizable $\langle\sigma\rangle$.

Detection and/or frequency filtering can be modelled with the formalism of frequency-filtered and time-resolved n -photon correlations [31], where the correlations of the filtered light are obtained as the quantum averages of a ‘‘sensor’’ taken in the limit of its vanishing coupling to the emitter, otherwise simply upgrading the Hamiltonian to

$$H = H_\sigma + \epsilon(a^\dagger \sigma + \sigma^\dagger a), \quad (18)$$

where a is the annihilation operator of an harmonic oscillator that models the sensor, which is ϵ -coupled to the emitter, and the master equation (8) gets an additional Lindblad term $(\Gamma/2)\mathcal{L}_a\rho$, which describes the bandwidth of the sensor and can be interpreted as the linewidth of an interference (Lorentzian-shaped) filter. In the steady-state and for a generic operator c , the second-order correlations are defined as [34]

$$g^{(2)}(\tau) = \frac{\langle c^\dagger(c^\dagger c)(\tau)c \rangle}{\langle c^\dagger c \rangle^2}, \quad (19)$$

and such quantities can be obtained for the sensor a according to the standard techniques, thereby providing easily quantities of direct and high experimental interest, such as those discussed in the main text (in particular $g^{(2)}(\tau)$ as shown in Fig. 3), without recourse to processing of the raw data. One quantity of great significance, and that can be obtained in this way, is the zero-delay two-photon correlator $g^{(2)}(0)$ at arbitrary driving Ω , which can be found by considering the cascaded excitation of an harmonic oscillator by the coherent single-photon source [32]. Defining $F_{kl} \equiv k\Gamma + l\gamma_\sigma$ for integers k, l (e.g., $F_{11} = \Gamma + \gamma_\sigma$), the two-photon coincidence correlation function is found as [32]:

$$g^{(2)}(\tau = 0) = \frac{F_{11}(\gamma_\sigma^2 + 4\Omega^2)(F_{11}F_{12} + 8\Omega^2)(48\Gamma^2\Omega^4 F_{21} + 4\Gamma\Omega^2 F_{31}(17\Gamma^3 + 29\Gamma^2\gamma_\sigma + 18\Gamma\gamma_\sigma^2 + 4\gamma_\sigma^3) + F_{11}F_{21}^2 F_{31}^2 F_{12}F_{32})}{F_{21}F_{31}(F_{11}F_{21} + 4\Omega^2)(F_{31}F_{32} + 8\Omega^2)(F_{12}F_{11}^2 + 4\Gamma\Omega^2)^2}. \quad (20)$$

This exact analytical expression describes with excellent accuracy the loss of antibunching observed in our experiment due to frequency filtering and taking into account anomalous correlations in the squeezing of the incoherent signal. This shows among other things that in the intermediate driving regime, $g^{(2)}(0)$ can be larger than 1, i.e., the coherently-driven two-level system can emit bunched filtered photons, in direct opposition to their previously assumed antibunched character.